

## Freezing of the Vortex Liquid in High- $T_c$ Superconductors: A Density-Functional Approach

Surajit Sengupta, C. Dasgupta,<sup>(a)</sup> H. R. Krishnamurthy,<sup>(a)</sup> Gautam I. Menon,  
and T. V. Ramakrishnan<sup>(a),(b)</sup>

*Department of Physics, Indian Institute of Science, Bangalore 560 012, India*

(Received 7 March 1991)

The structure of the unpinned vortex fluid in layered oxide high-temperature superconductors is investigated numerically using appropriate classical liquid-state theory, for magnetic fields  $B$  perpendicular to the layer plane. The direct correlation function so obtained is used as input for a first-principles, parameter-free calculation of the discontinuous fluid-to-Abrikosov-lattice transition boundary  $T_f(B)$ . This transition boundary is found to have a shape and location similar to that observed in strongly anisotropic materials, e.g., Bi-Sr-Ca-Cu-O.

PACS numbers: 74.60.Ge, 64.70.-p

There is overwhelming evidence by now for a relatively sharp transition in the mixed phase of high- $T_c$  oxide superconductors in a magnetic field [1-6]. The transition, crudely described as a change from solidlike to liquidlike behavior of interacting quantized magnetic-flux tubes, occurs at a boundary in the  $(H, T)$  plane well below the upper critical field  $H_{c2}(T)$ . Vortex entanglement and the resulting glassy state [7], a frozen defect-induced glass transition [8,9], thermal melting of the crystalline flux lattice [7,9-12], or rapid crossover from flux creep to flux flow [13] have all been proposed as explanations for this transition.

In this Letter, we report the results of the first, parameter-free statistical mechanical study of the vortex liquid structure and its first-order freezing transition into an Abrikosov lattice in the limit of vanishing interlayer Josephson coupling [14] and for the external magnetic field  $H$  parallel to the  $c$  axis. This transition should be seen in systems without frozen disorder for sufficiently slow cooling rates such that no glass transition intervenes. There is some evidence in very clean 1:2:3 systems of mild hysteretic effects characteristic of such first-order transitions [4]. Even if the vortex liquid forms a glass due to entanglement [7] or pinning [8,9], the thermodynamic liquid-crystalline solid boundary would underlie such a glass transition as in ordinary three-dimensional systems. Indeed, the observed "melting" curve for Bi-Sr-Ca-Cu-O single crystals [3], which have very weak interlayer Josephson coupling, is similar in shape and close in location to our freezing curve. Interestingly, the experimental transition seems insensitive to defect concentration [4].

Earlier suggestions of flux-lattice melting [7,9-12] have all been based on the Lindemann criterion which states that a solid melts when the rms thermal vibration amplitude of an atom is more than a certain fraction  $L$  of the interatomic spacing. This one-phase dimensionless criterion does not indicate why a first-order transition to a fluid phase occurs, and is quite mysterious since in typical isotropic 3D solids  $L \cong 0.1$ , a very small number. In the present context much larger values ( $\cong 0.3$ ) have been used, *ad hoc*, to obtain reasonable parameters. By contrast, we describe here a quantitative first-principles

theory of the vortex liquid and investigate the vortex-liquid-Abrikosov-lattice transition using density-functional theory, which has been successfully applied to study liquid-solid transitions in a wide variety of systems [15].

In the limit of zero interlayer Josephson coupling and for H||c, the vortex Hamiltonian assumes a particularly simple form which corresponds to a classical [16] system of point vortices of areal density  $\rho_A = B/\Phi_0$  (where  $B$  is the magnetic induction and  $\Phi_0 = hc/2e$  is the flux quantum), lying on the superconducting layers and interacting via an anisotropic pair potential [11] whose Fourier transform is given by

$$\beta V(\mathbf{k}) = \frac{\Gamma \lambda^2 [k_{\perp}^2 + (4/d^2) \sin^2(k_z d/2)]}{k_{\perp}^2 [1 + \lambda^2 k_{\perp}^2 + (4\lambda^2/d^2) \sin^2(k_z d/2)]} \quad (1)$$

Here,  $k_z$  ( $k_{\perp}$ ) is the component of the wave vector  $\mathbf{k}$  perpendicular (parallel) to the layers,  $d$  is the interlayer spacing,  $\lambda$  is the London penetration depth, and  $\Gamma$  is a dimensionless strength parameter given by  $\Gamma = \beta d \Phi_0^2 / 4\pi \lambda^2$ . Equation (1) implies that vortices lying on the same layer interact with the usual logarithmic repulsive potential, whereas vortices on different layers are coupled via an attractive potential arising from their magnetic interaction, this being weaker by a factor of  $d/\lambda \cong 0.01$ . This attraction favors point vortices on different layers lying directly on top of one another, forming vortex lines at low temperatures.

We have used standard liquid-state theory [17] to obtain the two-point correlation functions (Fig. 1) of this system. From these we have calculated the magnetic-field correlation function measured in neutron-scattering experiments (lower inset in Fig. 1). Using the calculated liquid-state direct correlation function  $c(r)$  in a density-functional theory [15], we obtain a first-order melting or freezing transition along a boundary in the  $(B, T)$  plane (Fig. 2). We emphasize that our theory does not contain any adjustable parameter and is a 3D theory, including fully the effects of the electromagnetic coupling between the layers.

We now proceed to describe the details of our calculation. As mentioned above, both intralayer and interlayer interactions between vortices in the present model are

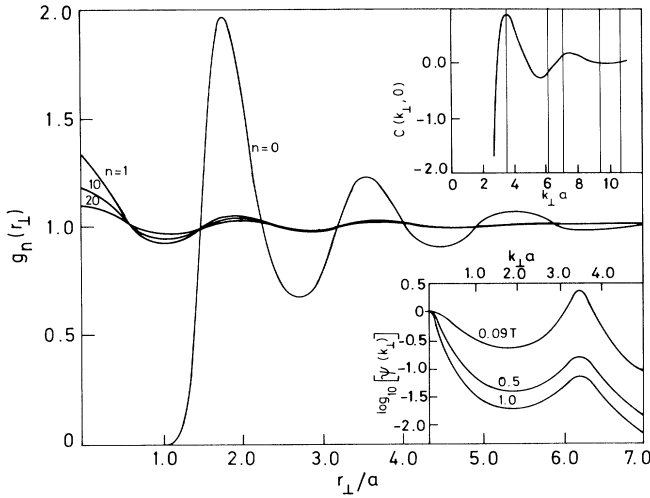


FIG. 1. Plot of the pair distribution function  $g_n(r_\perp)$  as a function of  $r_\perp/a$ , where  $a \equiv (\Phi_0/\pi B)^{1/2}$  (for comparison, the actual separation  $r_{nn}$  between nearest-neighbor vortices in the triangular lattice is  $1.9a$ ), for  $n=0, 1, 10$ , and  $20$  at  $T=30$  K and  $B=0.09$  T. Lower inset: Plot of the magnetic-field correlation function  $\Psi(k_\perp a)$  (defined in the text) as a function of  $k_\perp a$  at  $T=30$  K and  $B=1, 0.5$ , and  $0.09$  T. Note the logarithmic scale for  $\Psi$ . Upper inset: Plot of  $c(k_\perp, 0)$  vs  $k_\perp a$  for  $T=30$  K and  $B=0.085$  T. The light vertical lines mark the positions of the first few reciprocal-lattice vectors of the 2D triangular flux lattice.

smooth and long ranged. The intralayer interaction is large compared to  $k_B T$  ( $\Gamma \gg 1$ ). For classical liquids, it is well known [17] that with potentials of this type (e.g., in a one-component plasma) liquid-state correlation functions can be obtained adequately from a solution to the hypernetted chain (HNC) equation, a nonlinear self-consistent equation for the density distribution around a fixed atom. We have obtained the HNC equations that correspond to the present, layered case by replacing integrals over the  $z$  coordinate by a sum over  $n$ , the layer index. The resulting equations are

$$c_n(r_\perp) = \exp[-\beta V_n(r_\perp)] \exp[y_n(r_\perp)] - 1 - y_n(r_\perp), \quad (2a)$$

$$y(k_\perp, k_z) = \frac{c(k_\perp, k_z)}{1 - c(k_\perp, k_z)} - c(k_\perp, k_z), \quad (2b)$$

where  $r_\perp$  is the distance perpendicular to the  $z$  axis,  $c_n(r_\perp)$  is the Ornstein-Zernike direct correlation function [17] between two vortices separated by  $n$  layers and an in-plane distance  $r_\perp$ , and  $y_n(r_\perp) = g_n(r_\perp) - c_n(r_\perp) - 1$ ,  $g_n(r_\perp)$  being the pair distribution function. We use dimensionless Fourier transforms in Eq. (2b), e.g.,  $c(k_\perp, k_z)$  is the Fourier transform of  $c_n(r_\perp)$ .

A solution of the complete problem defined by the infinite set of Eqs. (2a) and (2b) is computationally difficult. However, when using the approximation  $c_n(r_\perp) = -\beta V_n(r_\perp)$  (the asymptotic result for large  $n$

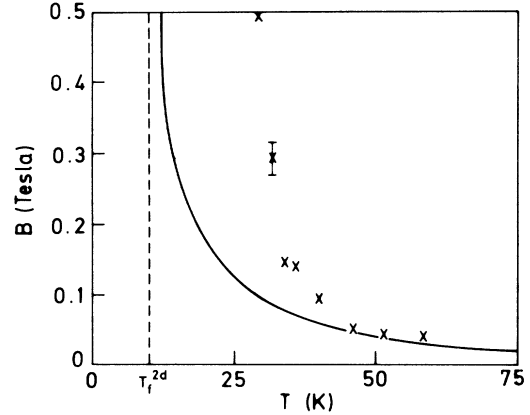


FIG. 2. The freezing line of the vortex liquid for the 2:2:1:2 compound. The solid curve is a guide to the eye and the dashed line denotes the asymptotic two-dimensional freezing temperature  $T_f^{2D} = 10$  K. For comparison, experimental results taken from Ref. [3] are shown as the crosses in the figure. The discrepancy with our calculation at low temperatures could be due to several factors discussed in the text. For example, a quite likely reduction of  $\lambda(0)$  from  $1500$  to  $1100$  Å can push the asymptotic (high  $B$ ) melting temperature up by a factor of 2 to  $\approx 25$  K in agreement with experiment.

and  $r_\perp$ ) for all  $n \neq 0$ , it is possible to integrate Eq. (2b) analytically over the variable  $k_z$  and to derive effective equations involving only  $c_0(r_\perp)$  and  $y_0(r_\perp)$ . The equations obtained in this limit were solved numerically [18], taking care to separate out the long- and the short-ranged pieces of  $c_0(r_\perp)$  [19]. At the end of the calculation, perturbative estimates of  $c_n(r_\perp)$  for  $n \neq 0$  over and above the asymptotic value  $-\beta V_n(r_\perp)$  were obtained by iterating the set of Eqs. (2a) and (2b) once. These were used to calculate  $g_n(r_\perp)$  for all  $n$ . The calculations show that our approximation for  $c_n(r_\perp)$  is excellent for almost all values of  $B$  and  $T$  for which the vortex liquid is the stable thermodynamic phase.

We have chosen in the parameters to correspond to those of the high- $T_c$  superconducting compound,  $\text{Bi}_2\text{-Sr}_2\text{CaCu}_2\text{O}_y$  (2:2:1:2) (viz.  $\lambda(0) = 1500$  Å,  $\lambda(T) = \lambda(0)/[1 - (T/T_c)^4]^{1/2}$ ,  $d = 15.26$  Å, and  $T_c = 85$  K) for all our calculations reported in this Letter. The resulting pair distribution function  $g_n(r_\perp)$  for a value of  $B$  ( $= 0.09$  T) close to the freezing transition (to be determined by a calculation described later) for  $T = 30$  K is shown in Fig. 1. Note the strong structure in  $g_0(r_\perp)$  generated by the "soft" potential (1), a well-known consequence of high densities and strong correlations [17]. It can be seen that for all  $n \neq 0$ ,  $g_n(r_\perp)$  has a peak at  $r_\perp = 0$ , which reflects the tendency of point vortices on adjacent layers to align. The correlations in the  $z$  direction decay exponentially with a correlation length  $\Lambda \cong \Lambda_1 B^{-1} + \Lambda_\infty$  in the liquid phase, where  $\Lambda_\infty/d \cong 5.5$  and  $\Lambda_1/d \cong 1.8$  T. This is a consequence of the screening of the interlayer electromagnetic coupling for large vortex densities.

We have also calculated the dimensionless magnetic-field correlation function given by

$$\Psi(k_{\perp}, k_z) = \beta \langle \mathbf{h}_{\mathbf{k}} \cdot \mathbf{h}_{-\mathbf{k}} \rangle / 4\pi V,$$

where  $\mathbf{h}(\mathbf{r})$  is the microscopic magnetic field,  $V$  is the total volume, and the angular brackets denote an ensemble average. This correlation function is proportional to the neutron-scattering intensity for scattering wave vector  $\mathbf{k}$ . For the case of  $k_z = 0$ , corresponding to scattering parallel to the layers, this is given by

$$\Psi(k_{\perp}) = \frac{\rho_A \Gamma \lambda^2}{(1 + \lambda^2 k_{\perp}^2)^2} S(k_{\perp}, 0), \quad (3)$$

where  $S(k_{\perp}, k_z)$  is the dimensionless structure factor of the vortex liquid. Our results for  $\Psi$  at  $T = 30$  K and at  $B = 1, 0.5$ , and  $0.09$  T are shown in the lower inset in Fig. 1 on a logarithmic scale. The peak at a finite wave number is a signature of liquid-state short-ranged order in the system and its height is seen to increase dramatically with decreasing  $B$ .

Finally, we have used the correlation functions calculated above as inputs to a density-functional theory of freezing [15]. In this theory the difference ( $\Omega_s - \Omega_l$ ) in the grand canonical free energy of a solid ( $s$ ) and a liquid ( $l$ ) is expressed as a functional of the single-particle density  $\rho(r)$ , the uniform liquid density being  $\rho_l$ . The simplest such functional has the form

$$\frac{\beta(\Omega_s - \Omega_l)}{N} = V^{-1} \int d^3r \frac{\rho(r)}{\rho_l} \left[ \ln \left( \frac{\rho(r)}{\rho_l} \right) - 1 \right] - \frac{1}{2} \sum_{\mathbf{G}} \rho_{\mathbf{G}}^2 c_{\mathbf{G}}. \quad (4)$$

In Eq. (4),  $\mathbf{G}$ 's are the reciprocal-lattice vectors (RLV's) of the crystalline solid,  $\rho_{\mathbf{G}}$ 's are the corresponding Fourier components of the solid density, and  $c_{\mathbf{G}} = c(\mathbf{k} = \mathbf{G})$ . The Fourier components  $\{\rho_{\mathbf{G}}\}$  of the density are varied so as to minimize the functional on the right-hand side of Eq. (4). The minimum corresponding to nonzero values for all  $\rho_{\mathbf{G}}$ 's represents the crystalline solid. The freezing condition is obtained when the solid and the liquid have the same free energy, i.e., for  $\Omega_s - \Omega_l = 0$ . External thermodynamic parameters (temperature, volume, etc.) enter the calculation through the dependence of the  $c_{\mathbf{G}}$ 's on them.

For the crystalline phase appropriate to the vortex system we consider here, i.e., the Abrikosov lattice, it is easy to show that  $\Omega_s - \Omega_l$  is given by a form identical to Eq. (4) with the RLV's  $\{\mathbf{G}\}$  corresponding to those of the *two-dimensional* triangular lattice and the set of numbers  $\{c_{\mathbf{G}}\}$  is given by  $c(k_{\perp}, k_z)$  calculated at  $|k_{\perp}| = |\mathbf{G}|$  and  $k_z = 0$  for a vortex liquid of areal density  $\rho_A$ . The integral in the first term in Eq. (4) can now be reduced to one over the area of a hexagonal unit cell in a single layer. The function  $c(k_{\perp}, 0)$  decays rapidly to zero for large  $k_{\perp}$  (see upper inset in Fig. 1); furthermore, for the two-dimensional system the order parameters  $\{\rho_{\mathbf{G}}\}$  tend to be

small and rapidly decreasing with increasing  $\mathbf{G}$ . This implies that the sum over  $\mathbf{G}$  in Eq. (4) is rapidly convergent. For this reason, a many-order-parameter calculation which we have carried out, retaining all  $c_{\mathbf{G}}$ 's, gives results close to those in which only the six  $c_{\mathbf{G}}$ 's corresponding to the smallest RLV set are retained.

Our many-order-parameter results for the phase diagram of the 2:2:1:2 compound are shown in Fig. 2. We obtain a first-order transition from a vortex liquid to the Abrikosov lattice for any given  $B$  at a temperature  $T_f(B)$ .  $\rho_{\mathbf{G}}$  at the smallest RLV jumps discontinuously from zero (liquid) to  $\approx 0.5$  (solid) across this phase boundary (in typical three-dimensional systems [15], the order parameter jumps are  $\approx 0.9$ ). The fractional change of the areal density at freezing is always less than 1%. We have calculated the Lindemann parameter  $L = \langle r^2 \rangle^{1/2} / r_{nn}$  in two ways, the first by exactly evaluating  $\langle r^2 \rangle$  over a unit cell with our density distribution  $\rho(\mathbf{r})$ , and the second by making a Gaussian approximation for the latter. Our values for  $L$  are 0.22 and 0.20, respectively, along the melting curve. These values are significantly lower than the empirical number of 0.3 used in Ref. [10] and much higher than the value ( $\sim 0.1$ ) typical of isotropic three-dimensional solids.

For large values of  $B$  the freezing temperature is expected [9,11,12] to approach that of a 2D system of point vortices. As shown in Fig. 2, the calculated freezing temperature becomes independent of  $B$  and approaches the value  $T_f^{2D}$  obtained from a separate density-functional calculation for a 2D system with a logarithmic potential, which is shown by the dashed line in Fig. 2. Molecular-dynamics simulations [20] of such a 2D system also show a first-order melting transition (with prominent hysteretic behavior) at  $\Gamma/2\pi \approx 140$ . The freezing temperature obtained in this simulation when translated into kelvins by using the parameters of the 2:2:1:2 compound yields  $T_f^{2D} \approx 15$  K which is somewhat higher than our value ( $\approx 10$  K). The discrepancy may partly be due to the HNC approximation which is known [17] to underestimate the size of the fluid-state correlations.

The first-order melting curve is similar in shape [21] and location to the observed continuous transition [3] (see Fig. 2 for comparison with data). However, the latter occurs at somewhat higher temperatures for the same field  $B$  especially in the large field regime. There are several possible reasons for this, e.g., the HNC approximation, large uncertainties in the absolute scale of  $\Gamma$  traceable to that in  $\lambda$ , neglect of Josephson coupling, and, finally, the comparison of a glass transition boundary with an underlying thermodynamic transition occurring in a clean, nonentangled flux system. Furthermore, experimental results are quoted in terms of  $H$  (the externally applied field), whereas it is the magnetic induction  $B$  which controls the vortex density that enters our calculation directly.

Important extensions of the present calculation would be the inclusion of the interlayer Josephson coupling and

of random pinning. The effect of the former is to generate an interaction between point vortices on nearest-neighbor planes, of range  $r_{\perp} \cong \lambda$  and integrated strength  $\Gamma(\xi_c/\xi_{ab})^2$ . The fluid-state correlations for weak short-range random pinning can be investigated using a replica density-functional theory. These effects are currently under investigation.

The authors would like to thank Sriram Ramaswamy for useful discussions and P. Vashishta for pointing out Ref. [20]. S.S. and G.I.M. would like to thank the Council for Scientific and Industrial Research (India) for financial support.

<sup>(a)</sup>Also at Jawaharlal Nehru Center for Advanced Scientific Research, Bangalore, India.

<sup>(b)</sup>Present address: Joseph Henry Laboratories of Physics, Princeton University, Princeton, NJ 08544.

- [1] K. A. Muller, M. Takashige, and J. G. Bednorz, *Phys. Rev. Lett.* **58**, 1143 (1987); A. P. Malozemoff *et al.*, *Phys. Rev. B* **38**, 7203 (1988).
- [2] P. L. Gammel *et al.*, *Phys. Rev. Lett.* **61**, 1666 (1988).
- [3] C. Duran, J. Yazzi, F. de la Cruz, D. J. Bishop, D. B. Mitzi, and A. Kapitulnik, *Phys. Rev. B* **44**, 7737 (1991).
- [4] T. K. Worthington, F. Holtzberg, and C. A. Feild, *Cryogenics* **30**, 417 (1990).
- [5] R. H. Koch *et al.*, *Phys. Rev. Lett.* **63**, 1511 (1989); R. H. Koch, V. Voghettis, and M. P. A. Fisher, *Phys. Rev. Lett.* **64**, 2586 (1990); P. L. Gammel, L. F. Schneemayer, and D. J. Bishop, *Phys. Rev. Lett.* **66**, 953 (1991).
- [6] D. R. Harshman *et al.*, *Phys. Rev. Lett.* **66**, 3313 (1991).
- [7] D. R. Nelson and S. Seung, *Phys. Rev. B* **39**, 9153 (1989); M. C. Marchetti and D. R. Nelson, *Phys. Rev. B* **41**, 1910 (1990).
- [8] M. P. A. Fisher, *Phys. Rev. Lett.* **62**, 1415 (1989).
- [9] D. S. Fisher, M. P. A. Fisher, and D. A. Huse, *Phys. Rev. B* **43**, 130 (1991).
- [10] A. Houghton, R. A. Pelcovits, and A. Sudbo, *Phys. Rev. B* **40**, 6763 (1989); E. H. Brandt, *Phys. Rev. Lett.* **63**, 1106 (1989).
- [11] M. V. Feigel'man, V. B. Geshkenbeing, and A. I. Larkin, *Physica (Amsterdam)* **167C**, 177 (1990).
- [12] L. I. Glazman and A. F. Koshelev, *Phys. Rev. B* **43**, 2835 (1991).
- [13] E. H. Brandt, *Int. J. Mod. Phys. B* **5**, 751 (1991).
- [14] All the qualitative properties of vortex lines, e.g., a non-vanishing tilt modulus of an isolated vortex line or the shear modulus for the Abrikosov lattice, are present in this limit, because of (electro)magnetic coupling between point vortices on different layers. The limit is even quantitatively accurate for weak interlayer coupling (e.g., as in Bi-Sr-Ca-Cu-O) or at high magnetic fields [12].
- [15] T. V. Ramakrishnan and M. Youssouf, *Phys. Rev. B* **19**, 2775 (1979). See D. W. Oxtoby, in *Liquids, Freezing and the Glass Transition*, edited by J. P. Hansen, D. Levesque, and J. Zinn-Justin (North-Holland, Amsterdam, 1990), for a recent review.
- [16] The classical approximation used by us should be accurate because (a) the motion of a vortex is dissipative and (b) the dimensionless quantum statistical parameter is  $\hbar\omega_c^*/k_B T$ , where  $\omega_c^* = (eB/m^*c)$ ,  $m^*$  being the vortex effective mass per layer (approximately equal to the normal core). This is very small except at very low temperatures and high magnetic fields.
- [17] See, for example, J. P. Hansen and I. R. Macdonald, *Theory of Simple Liquids* (Academic, London, 1986), 2nd ed.; in particular, see J. P. Hansen and D. Levesque, *J. Phys. C* **14**, L603-608 (1981).
- [18] M. J. Gillan, *Mol. Phys.* **38**, 6 (1979); **38**, 1781 (1979).
- [19] F. Lado, *Phys. Rev. B* **17**, 7 (1978); **17**, 2827 (1978).
- [20] P. Choquard and C. Clerouin, *Phys. Rev. Lett.* **50**, 2086 (1983); S. W. de Leeuw and J. W. Perram, *Physica (Amsterdam)* **113A**, 546 (1982); J. M. Caillol, D. Levesque, J. J. Weis, and J. P. Hansen, *J. Stat. Phys.* **28**, 325 (1982).
- [21] A crude idea of the shape of the melting curve can be obtained by generalizing the "2D" melting criterion  $\Gamma/2\pi = \beta\Phi_0^2 d/8\pi^2\lambda^2 \geq 141$ . Making the obvious replacement of  $d$  by  $\Lambda$ , where  $\Lambda$  is the  $z$ -axis correlation length discussed above, and using the relation  $\Lambda = \Lambda_1 B^{-1} + \Lambda_\infty$ , as well as the temperature dependence of  $\lambda$ , a curve resembling Fig. 2 is obtained.